

Protection against peroxynitrite-induced DNA damage by mesalamine: implications for anti-inflammation and anti-cancer activity

By: Paul M. Graham, Jason Z. Li, Xueqing Dou, Hong Zhu, Hara P. Misra, [Zhenquan Jia](#), Yunbo Li

Graham PM, Li JZ, Dou X, Zhu H, Misra HP, Jia Z, Li Y. Protection against peroxynitrite-induced DNA damage by mesalamine: implications for anti-inflammation and anti-cancer activity. *Mol Cell Biochem*, 378(1-2):291-8, 2013.

The final publication is available at Springer via <http://dx.doi.org/10.1007/s11010-013-1620-z>

***© Springer. Reprinted with permission. No further reproduction is authorized without written permission from Springer. This version of the document is not the version of record. Figures and/or pictures may be missing from this format of the document. ***

Abstract:

Mesalamine (5-aminosalicylic acid, 5-ASA) is known to be the first-line medication for treatment of patients with ulcerative colitis. Studies have demonstrated that ulcerative colitis patients treated with 5-ASA have an overall decrease in the risk of developing colorectal carcinoma. However, the mechanisms underlying 5-ASA-mediated anti-inflammatory and anti-cancer effects are yet to be elucidated. Because peroxynitrite has been critically involved in inflammatory stress and carcinogenesis, this study was undertaken to investigate the effects of 5-ASA in peroxynitrite-induced DNA strand breaks, an important event leading to peroxynitrite-elicited cytotoxicity. Incubation of ϕ X-174 plasmid DNA with the peroxynitrite generator 3-morpholinopyrrolidine (SIN-1) led to the formation of both single- and double-stranded DNA breaks in a concentration-dependent manner. The presence of 5-ASA at 0.1 and 1.0 mM was found to significantly inhibit SIN-1-induced DNA strand breaks in a concentration-dependent manner. The consumption of oxygen induced by SIN-1 was found to not be affected by 5-ASA at 0.1–50 mM, indicating that 5-ASA at these concentrations is not involved in the auto-oxidation of SIN-1 to form peroxynitrite. It is observed that 5-ASA at 0.1–1 mM showed considerable inhibition of peroxynitrite-mediated luminol chemiluminescence in a dose-dependent fashion, suggesting that 5-ASA is able to directly scavenge the peroxynitrite. Electron paramagnetic resonance (EPR) spectroscopy in combination with spin-trapping experiments, using 5,5-dimethylpyrroline-*N*-oxide (DMPO) as spin trap resulting in the formation of DMPO-hydroxyl radical adduct from peroxynitrite, and 5-ASA only at higher concentration (1 mM) inhibited the hydroxyl radical adduct while shifting EPR spectra, indicating that 5-ASA at higher concentrations may generate a more stable free radical species rather than acting purely as a hydroxyl radical scavenger. Taken together, these studies demonstrate for the first time that 5-ASA can potentially inhibit peroxynitrite-mediated DNA strand breakage, scavenge peroxynitrite,

and affect peroxynitrite-mediated radical formation, which may be responsible, at least partially, for its anti-inflammatory and anti-cancer effects.

Abbreviations

DMPO: 5,5-Dimethylpyrroline-N-oxide

EPR: Electron paramagnetic resonance

SIN-1: 3-Morpholinopyrrolidine

5-ASA: 5-Aminosalicylic acid (mesalamine)

PBS: Phosphate-buffered saline

NaHCO₃: Sodium bicarbonate

Keywords: Peroxynitrite | Mesalamine | DNA strand breaks | SIN-1 | Anti-inflammation and anti-cancer activity

Article:

Introduction

The incidence of ulcerative colitis has been steadily increasing worldwide [1]. Ulcerative colitis is a chronic inflammatory bowel disease characterized by chronic and widespread inflammation of the colorectal mucosa. Patients with chronic ulcerative colitis are at an increased risk of developing colorectal carcinoma and have a higher frequency of multiple synchronous colorectal cancers [2, 3], which remains the third leading cause of cancer-related death in both men and women of the United States [4]. As such, chronic inflammation has been suggested to be involved in both steps of initiation and propagation of carcinogenesis, which represents a major risk factor for the development of colorectal cancer [5, 6]. Mesalamine (5-aminosalicylic acid, 5-ASA) is currently the first-line medication for patients suffering from ulcerative colitis and for maintenance of the disease after remission (Fig. 1). 5-ASA has been proved to be very well tolerated and remains the gold standard pharmacological intervention for patients with mild to moderate ulcerative colitis. Interestingly, studies showed that there is a significant association between the use of 5-ASA and the reduction in incidence of colorectal carcinoma [7]. Among those subjects with ulcerative colitis who did not develop colorectal carcinoma, it was found that 100 % used 5-ASA to induce remission. This is in comparison to those with ulcerative colitis who developed colorectal carcinoma—only 76.9 % of these individuals used 5-ASA [7]. Although a protective role for 5-ASA against the development of colorectal carcinoma in the patients with ulcerative colitis has been shown epidemiologically [8–10], the molecular mechanism for its anti-cancer and anti-inflammation activity remains unknown.

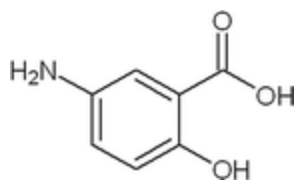


Fig. 1 Structure of mesalamine (5-ASA)

Peroxynitrite, a strong oxidant anion (ONOO^-), has been increasingly recognized as a pivotal mechanism contributing to the progression of many chronic diseases, including cancer, and many neurodegenerative diseases [11–14]. Peroxynitrite is generated from the bi-radical reaction of nitric oxide and superoxide at a diffusion-limited rate at physiologic pH [15]. Peroxynitrite can react directly with numbers of biologic targets such as proteins, phospholipids, and DNA to produce various covalent adducts leading to the propagation and amplification of human cancer [11]. Multiple mechanisms account for the cytotoxicity elicited by peroxynitrite. Among them, DNA strand breakage and the subsequent poly (ADP-ribose) polymerase activation have been demonstrated to be critical events [16]. In this context, cellular DNA is an important target for peroxynitrite attack and peroxynitrite can predominantly cause DNA damage to induce DNA strand breaks and form 8-nitroguanine and 8-oxoguanine DNA adduct [17]. Because peroxynitrite has been associated with increased oxidative reactions and DNA damage in multistage carcinogenesis, in this study, using $\phi\text{X-174}$ plasmid DNA as a model system, we investigated the effects of 5-ASA on peroxynitrite-induced DNA strand breaks. We observed that 5-ASA at pharmacologically relevant concentrations significantly inhibited peroxynitrite-mediated oxidative DNA cleavage as well as peroxynitrite-mediated luminol chemiluminescence, which may be responsible, at least partially, for its epidemiologically protective activities against inflammation-mediated colorectal carcinoma.

Materials and methods

Materials

$\phi\text{X-174}$ RF I plasmid DNA was from New England Biolabs (Beverly, MA). Phosphate-buffered saline (PBS, pH 7.4) was from Gibco Life Technologies, Grand Island, NY. 3-Morpholinosydnonimine (SIN-1) and other chemicals were from Sigma Chemical (St. Louis, MO). PBS was prepared in the lab. Peroxynitrite was from Enzo Life Sciences (Farmingdale, NY).

Preparation of SIN-1 and peroxynitrite

SIN-1 was dissolved in phosphate buffer saline (pH 5.5), and stored at $-80\text{ }^\circ\text{C}$. The concentration of peroxynitrite was determined spectrophotometrically at 302 nm (extinction coefficient = $1670\text{ M}^{-1}\text{ cm}^{-1}$). The peroxynitrite was an aliquot and stored at $-80\text{ }^\circ\text{C}$.

Assay for DNA strand breaks

DNA strand breaks were measured by the conversion of supercoiled ϕ X-174 RF I double-stranded DNA to open circular and linear forms [18]. Briefly, 0.3 μ g DNA was incubated with SIN-1 in the presence or absence of 5-ASA at 37 °C in phosphate-buffered saline (pH 7.4) at a final volume of 24 μ l. Following incubation, loading dye was added and the samples were immediately loaded in a 1 % agarose gel, containing 40 mM Tris, 20 mM sodium acetate, and 2 mM EDTA, and electrophoresed in a horizontal slab gel apparatus in Tris/acetate/EDTA gel buffer. After electrophoresis, the gels were stained with 20 μ l of SYBR green I nucleic acid stain in 200 ml solution of Tris/acetate/EDTA for 30 min. The gel was then photographed under ultraviolet illumination and quantified using an Alpha Innotech Imaging system (San Leandro, CA).

Measurement of oxygen consumption

Oxygen consumption caused by SIN-1 auto-oxidation was monitored with a Clark oxygen electrode (YSI 5300, Yellow Springs, OH) upon mixing SIN-1 with 5-ASA in 2.5 ml air-saturated phosphate-buffered saline (pH 7.40) at 37 °C. The reaction was run at 30-min intervals for three trials. The oxygen consumption was expressed as percentage of oxygen consumed [19]. The reagents were mixed according to the following experimental conditions: (1) SIN-1 + PBS; (2) SIN-1 + PBS + 5-ASA; (3) SIN-1 + PBS/sodium bicarbonate (NaHCO_3); (4) SIN-1 + PBS/ NaHCO_3 + 5-ASA. 5-ASA was introduced incrementally into the 250 μ M SIN-1 + PBS solution for three trials at concentrations 0.01, 0.1, 1.0, and 50 mM.

Peroxynitrite-induced luminol chemiluminescence

Chemiluminescence was measured with a Berthold Biolumat LB9505C Luminometer (Germany). Chemiluminescence was conducted at 37 °C for 60 min. The results were determined with a data analysis program supplied with the luminometer. The data are presented in cumulative counts for 60 min per trial. The reaction mixture contained 250 μ M SIN-1 in 1 ml freshly prepared phosphate buffer solution in the presence or absence of varying concentrations of 5-ASA. To initiate the luminal-derived chemiluminescence, 10 μ M luminol was added to the mixture. 5-ASA was added to each mixture at increasing concentrations of 0.01, 0.1, and 1.0 mM. The data acquired from each experiment were articulated as the area under the curve, expressed as the integral in each dataset.

Electron paramagnetic resonance spin-trapping assay

Spin trap 5,5-dimethylpyrroline-*N*-oxide (DMPO) was used to measure hydroxyl radical formation generated by the addition of peroxynitrite in the presence of varying concentrations of 5-ASA. To measure the reactive oxygen species produced, the electron paramagnetic resonance (EPR) spectra were recorded at room temperature with a spectrometer (Bruker D-200 ER, IBM-Bruker), operating at X-band with a TM cavity and capillary cell. The spectrometer settings were as follows: modulation frequency, 86 kHz; microwave frequency, 9.845 GHz; microwave power, 29.8 mW; modulation amplitude 2.17 G; and scan time, 400 s. Reactants were mixed in test

tubes to a final volume of 0.2 ml following transfer to a capillary cell for EPR spectral studies at room temperature under conditions described above.

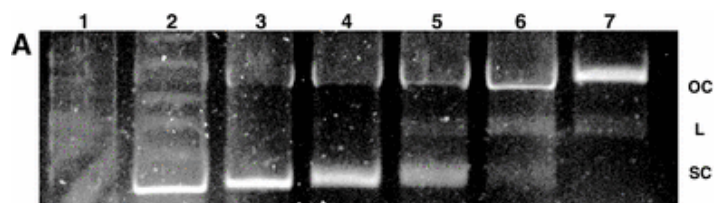
Statistical analyses

Analysis of variance was used. Further statistical analyses for post hoc comparisons were performed using the Student two-tailed *t* test. All differences of $p \leq 0.05$ were considered significant in this investigation.

Results/discussion

Induction of DNA strand breaks by SIN-1

Induction of single-strand and double-strand breaks of supercoiled ϕ X-174 RF I plasmid DNA leads to the formation of open circular and linear forms [20]. Double-strand breaks are indicative of the linear form and single-strand breaks are indicative of the open circular form of DNA [20]. At a physiologic pH, SIN-1 generates peroxynitrite from auto-oxidation to produce equal molar superoxide and nitric oxide, and this auto-oxidation leads to the formation of peroxynitrite [21]. As such, SIN-1 is routinely used as a peroxynitrite generator to investigate the effects of peroxynitrite-induced DNA damage in vitro [22]. As shown in Fig. 2, incubation of the plasmid DNA with 25–500 μ M SIN-1 at 37 °C for 30 min demonstrated significant single-strand and double-strand DNA breaks as evidenced by the formation of open circular and linear DNA bands. These results indicate that SIN-1 was able to elicit both single- and double-stranded breaks in this plasmid DNA system, which is consistent with our previous report [18].



Lane 1: Marker
Lane 2: Control
Lane 3: SIN-1 25 μ M
Lane 4: SIN-1 50 μ M
Lane 5: SIN-1 100 μ M
Lane 6: SIN-1 250 μ M
Lane 7: SIN-1 500 μ M

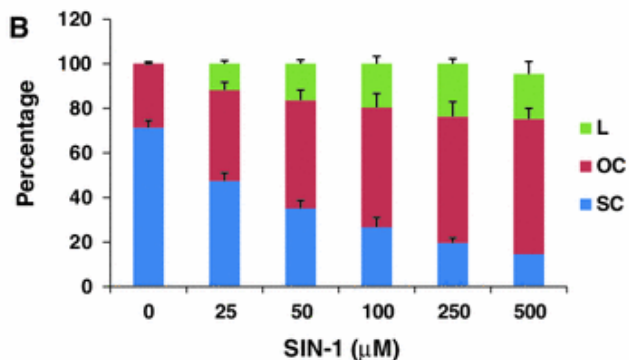


Fig. 2 Concentration-dependent induction of DNA strand breaks by SIN-1 in the ϕ X-174 plasmid DNA. The marker used was lambda DNA-*Hind*III digest. *OC*, *L*, and *SC* stand for open circular, linear, and supercoiled DNA, respectively. **a** is a representative gel picture of ϕ X-174 RF I plasmid DNA following incubation at 37 °C for 30 min with increasing concentration of SIN-1. **b** represents the percentage of supercoiled, open circular, and linear forms of DNA after incubation with increasing concentrations of SIN-1. These data represent the averages of three independent trials

Inhibition of SIN-1-induced DNA strand breaks by 5-ASA

A significant formation of open circular and linear forms of DNA was observed following incubation of plasmid DNA with 250 μ M SIN-1 for 30 min (Fig. 2); thus, we chose to select the 250 μ M SIN-1 as the representative concentration for investigation of the protective effects of 5-ASA under the same conditions. As demonstrated by Fig. 3, the SIN-1-mediated single- and double-stranded DNA breaks were markedly reduced by 5-ASA in a concentration-dependent manner. In the presence of 5-ASA at 0.1 and 1.0 mM, the SIN-1-mediated conversion of supercoiled DNA to both open circular and linear forms was markedly reduced (Fig. 3), indicating that 5-ASA was able to protect against SIN-1-induced DNA strand breaks, including both single-stranded and double-stranded cleavage.

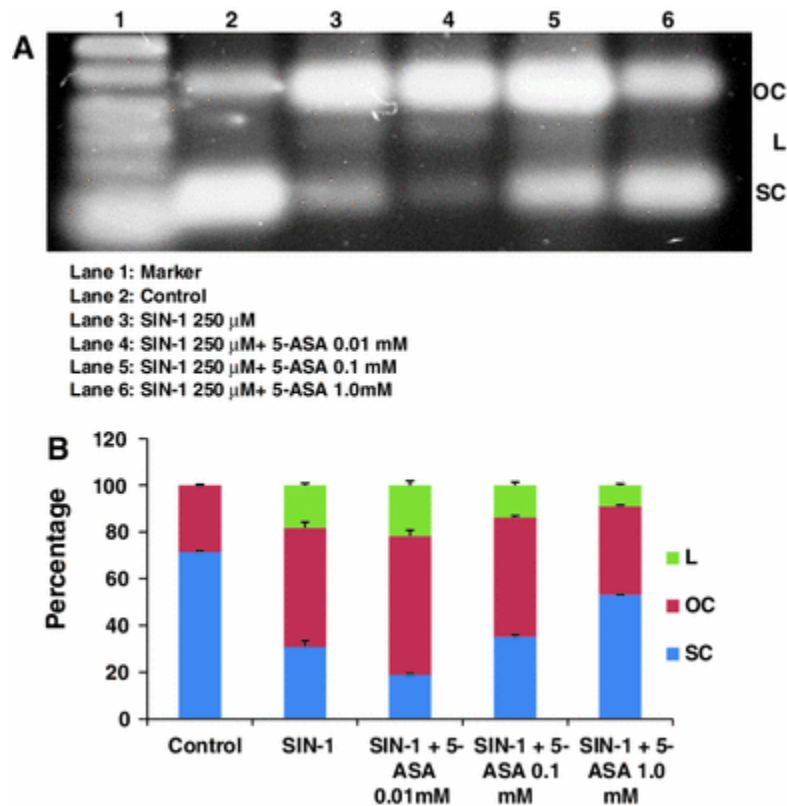


Fig. 3 Inhibitory effects of 5-ASA on SIN-1-induced DNA strand breaks in the ϕ X-174 plasmid DNA. The plasmid DNA was incubated with SIN-1 in the presence or absence of the indicated

concentrations of 5-ASA for 30 min. *OC*, *L*, and *SC* stand for open circular, linear, and supercoiled DNA, respectively. **a** is a representative gel picture. **b** The concentration of SIN-1 was 250 μM . These data represent the averages of three independent trials

Effects of 5-ASA on SIN-1-mediated oxygen consumption

Because auto-oxidation of SIN-1 is a critical step in formation of peroxynitrite, one potential mechanism involved in the protective effects of 5-ASA against SIN-1-induced DNA strand breaks could be due to the direct inhibitory effect of 5-ASA on the auto-oxidation of SIN-1, thereby diminishing peroxynitrite-induced DNA damage. In order to investigate this potential protective mechanism, we investigated the effects of 5-ASA on SIN-1-mediated oxygen utilization. As shown in Fig. 4a, SIN-1 at 250 μM resulted in oxygen consumption by 20 % in PBS (pH 7.4) 30 min after the addition of SIN-1. However, 5-ASA at 0.01–50 mM was not found to significantly affect the oxygen consumption by 250 μM SIN-1 (Fig. 4b). It has become increasingly evident that carbon dioxide plays a critical role in the formation of the peroxynitrite during SIN-1 auto-oxidation as it can directly react with peroxynitrite [19]. Thus, we further examined the effects of bicarbonate on SIN-1-mediated oxygen consumption in the presence of 5-ASA. As shown in Fig. 5a, PBS containing NaHCO_3 solution in the presence of 250 μM SIN-1 resulted in significant oxygen consumption by 60 % compared to the PBS only solution (Fig. 4a). The higher oxygen consumption may be due to an increase in pH with the presence of NaHCO_3 (pH 8.8). The addition of NaHCO_3 in the phosphate buffer solution acts to increase the pH of the reaction mixture, thus speeding up the rate of the reaction of SIN-1 auto-oxidation. As shown in Fig. 5b, 5-ASA at 0.01–50 mM did not significantly affect the oxygen consumption in PBS containing NaHCO_3 solution, indicating that 5-ASA is not involved in preventing the auto-oxidation of SIN-1 to form peroxynitrite in solution.

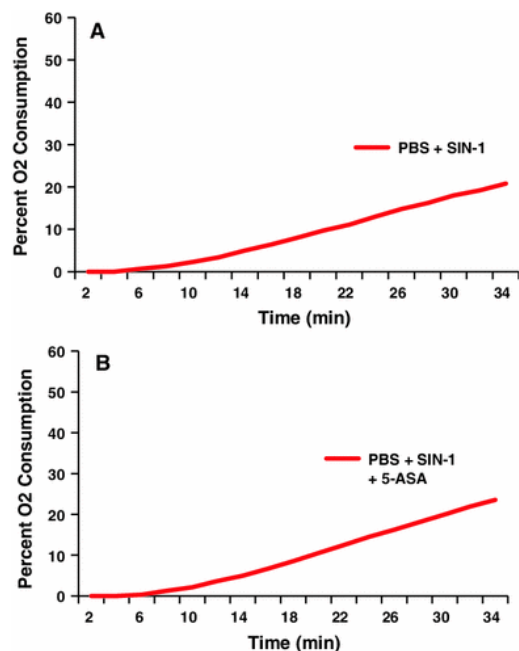


Fig. 4 Effects of 5-ASA on SIN-1-mediated oxygen consumption in PBS solution (pH 7.40). The oxygen consumption was measured following incubation of SIN-1 in the presence or absence of 50 mM 5-ASA for 30 min in PBS solution (pH 7.4). **a** represents oxygen consumption curves with 250 μ M SIN-1. **b** represents the effect of 5-ASA on oxygen consumption caused by 250 μ M SIN-1. These data are representative of the mean \pm SEM from three independent experiments

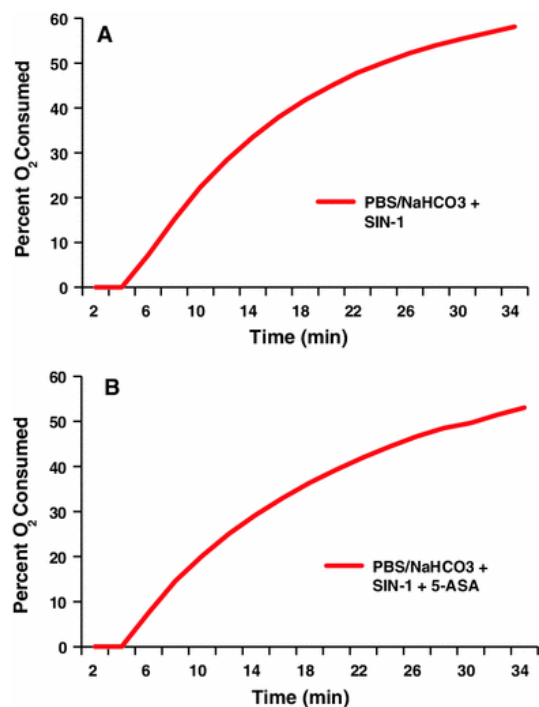
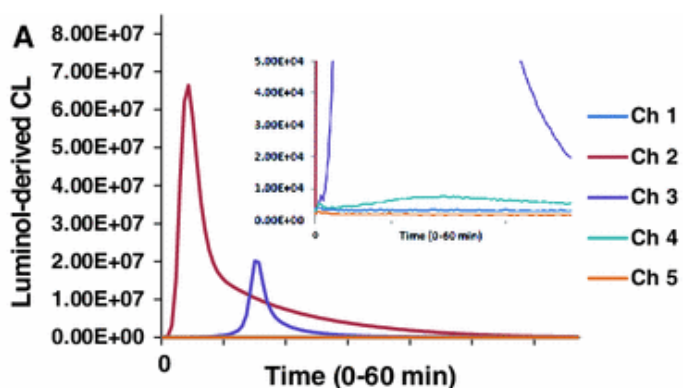


Fig. 5 Effects of 5-ASA on SIN-1-mediated oxygen consumption in PBS containing NaHCO₃ solution (pH 8.8). The oxygen consumption was measured following incubation of SIN-1 in the presence or absence of 50 mM 5-ASA for 30 min in PBS containing NaHCO₃ solution (pH 8.8). **a** represents oxygen consumption curves with 250 μ M SIN-1. **b** represents the effect of 5-ASA on oxygen consumption caused by 250 μ M SIN-1. These data are representative of the mean \pm SEM from three independent experiments

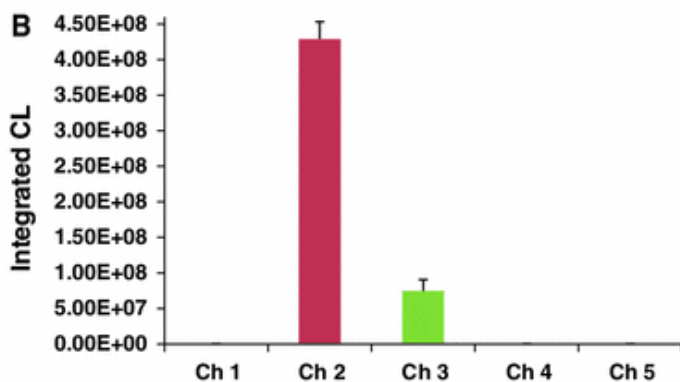
Effects of 5-ASA on SIN-1-mediated peroxynitrite production measured by luminol chemiluminescence: potential protective mechanisms

To further explore the potential mechanism that may exist underlying the protective effect of 5-ASA against SIN-1-mediated DNA breaks, we further investigated if 5-ASA could directly scavenge the peroxynitrite, thus contributing to the protection against SIN-1-induced DNA strand breaks. Previous studies have demonstrated that luminol-derived chemiluminescence is a highly sensitive method for studying the effect of biologic antioxidants on the peroxynitrite-mediated light reaction, and SIN-1-induced luminol luminescence is mainly due to the action of peroxynitrite [23, 24]. The production of light depends on luminol decomposition during the reaction with peroxynitrite [25]. Figure 6, channel 1, demonstrates that no chemiluminescence is

emitted in the absence of SIN-1 indicating that luminol is not able to undergo oxidation, therefore causing no light to be produced. Upon addition of 250 μM SIN-1 to the PBS containing NaHCO_3 solution (pH 8.8), a steep peak is observed within the first 5 min of the measurement (Fig. 6, Channel 2). As demonstrated in Fig. 6, panel a, channels 3–5, the addition of 5-ASA caused a dose-dependent inhibition of luminol chemiluminescence. It is noteworthy that the addition of 0.1 and 1.0 mM 5-ASA almost completely eliminated the chemiluminescence peak in comparison to the control, indicating the peroxynitrite-scavenging activity of 5-ASA. As shown in Fig. 7, the addition of increasing concentrations of 5-ASA also inhibits peroxynitrite-mediated luminol chemiluminescence with the same effect in a PBS solution (without NaHCO_3). However, as compared to Fig. 6 in a PBS + NaHCO_3 containing solution, the PBS only solution demonstrated a 20-fold decrease in chemiluminescence signal intensity (Fig. 7), indicating that chemiluminescence is pH dependent. When bicarbonate is added to the reaction mixture (pH 7.4), it raises the pH of the solution to 8.8. It has been shown that the rise in pH facilitates the oxidation of luminol to form the emitting species, aminophthalate, thus yielding a greater chemiluminescence peak [26].

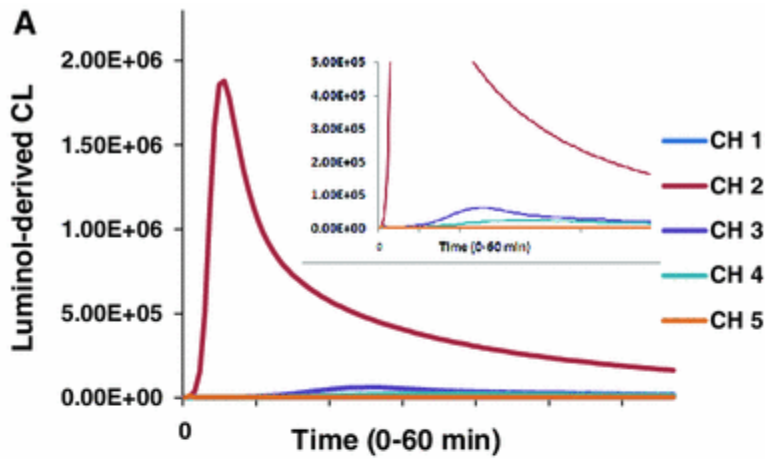


Channel 1: PBS + NaHCO_3 + Luminol 10 μM
 Channel 2: PBS + NaHCO_3 + Luminol 10 μM + SIN-1 250 μM
 Channel 3: PBS + NaHCO_3 + Luminol 10 μM + SIN-1 250 μM + 5-ASA 0.01 mM
 Channel 4: PBS + NaHCO_3 + Luminol 10 μM + SIN-1 250 μM + 5-ASA 0.1 mM
 Channel 5: PBS + NaHCO_3 + Luminol 10 μM + SIN-1 250 μM + 5-ASA 1.0 mM

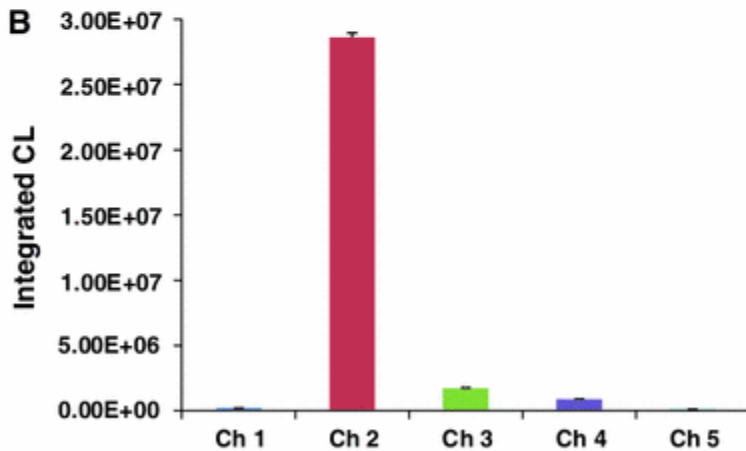


Channel 1: PBS + NaHCO_3 + Luminol 10 μM
 Channel 2: PBS + NaHCO_3 + Luminol 10 μM + SIN-1 250 μM
 Channel 3: PBS + NaHCO_3 + Luminol 10 μM + SIN-1 250 μM + 5-ASA 0.01 mM
 Channel 4: PBS + NaHCO_3 + Luminol 10 μM + SIN-1 250 μM + 5-ASA 0.1 mM
 Channel 5: PBS + NaHCO_3 + Luminol 10 μM + SIN-1 250 μM + 5-ASA 1.0 mM

Fig. 6 Inhibitory effects of 5-ASA on peroxyxynitrite-induced luminal chemiluminescence in PBS containing NaHCO₃ solution (pH 8.8). SIN-1 (250 μM) was added to reaction mixture containing 10 mM luminol and increasing concentrations of 5-ASA (0.01, 0.1, and 1.0 mM) in PBS NaHCO₃ containing solution (pH 8.80) at 37 °C for 60 min. **a** Luminol-derived chemiluminescence signal intensity was observed and recorded as a function of increasing concentrations of 5-ASA in channels 3–5. **b** Integrated chemiluminescence of all three trials with increasing concentrations of 5-ASA in a PBS + NaHCO₃ containing solution. These data are representative of the mean ± SEM from three independent experiments. * *p* < 0.05 versus SIN-1 250 μM only (channel 2)



Channel 1: PBS + Luminol 10 μM
 Channel 2: PBS + Luminol 10 μM + SIN-1 250 μM
 Channel 3: PBS + Luminol 10 μM + SIN-1 250 μM + 5-ASA 0.01 mM
 Channel 4: PBS + Luminol 10 μM + SIN-1 250 μM + 5-ASA 0.1 mM
 Channel 5: PBS + Luminol 10 μM + SIN-1 250 μM + 5-ASA 1.0 mM



Channel 1: PBS + Luminol 10 μM
 Channel 2: PBS + Luminol 10 μM + SIN-1 250 μM
 Channel 3: PBS + Luminol 10 μM + SIN-1 250 μM + 5-ASA 0.01 mM
 Channel 4: PBS + Luminol 10 μM + SIN-1 250 μM + 5-ASA 0.1 mM
 Channel 5: PBS + Luminol 10 μM + SIN-1 250 μM + 5-ASA 1.0 mM

Fig. 7 Inhibitory effects of 5-ASA on peroxynitrite-induced luminal chemiluminescence in PBS solution (pH 7.4). SIN-1 (250 μ M) was added to reaction mixture containing 10 mM luminol and increasing concentrations of 5-ASA (0.01, 0.1, and 1.0 mM) in PBS solution (pH 7.4) at 37 $^{\circ}$ C for 60 min. **a** Luminol-derived chemiluminescence signal intensity was observed and recorded as a function of increasing concentrations of 5-ASA in channels 3–5. **b** Integrated chemiluminescence with increasing concentrations of 5-ASA in a PBS solution. These data are representative of the mean \pm SEM from three independent experiments. * $p < 0.05$ versus SIN-1 250 μ M only (channel 2)

Effect of 5-ASA on peroxynitrite-mediated generation of hydroxyl radicals

It has been demonstrated that decomposition of peroxynitrite leads to the generation of oxidant/radical species that can damage a wide array of molecules in cells, including nucleic acids [27]. As such, the EPR spin-trapping technique was employed to study the effects of 5-ASA on the generation of peroxynitrite-mediated free radicals. DMPO-spin trap was employed to produce more stable spin adducts from the reaction between the DMPO, superoxide, and hydroxyl radicals [28]. As shown in Fig. 8, decomposition of peroxynitrite in the presence of DMPO led to the formation of a DMPO spin adduct with the hyperfine splitting constants of $a_N = a_H = 14.9$ G representative of DMPO-hydroxyl adduct (DMPO-OH) [29]. DMPO itself did not give rise to the formation of any distinct spectra (Fig. 8 line a), indicating the high purity of the spin trap used in this study. It has been showed that the hydroxyl radical spin adduct, DMPO-OH, could also be derived from decomposition of the superoxide spin adduct (DMPO-OOH) [30]. However, our previous studies have demonstrated that the addition of SOD did not affect the EPR signal intensity of DMPO-OH, indicating that the DMPO trapping of hydroxyl radicals during the decomposition of peroxynitrite in this experiment does not form decomposition of the superoxide spin adduct (DMPO-OOH) [31]. It is observed that the addition of increasing concentrations of the DMPO-OH spin adduct signal is not inhibited by 5-ASA at 0.01 and 0.1 mM, indicating that 5-ASA at low concentrations does not effectively scavenge the \cdot OH radical produced. Interestingly, 5-ASA at 1 mM was found to inhibit hydroxyl radical adduct, while shifting EPR spectra of DMPO spin adduct. This spectra shift indicates that 5-ASA at higher concentrations in the reaction mixture may generate a more stable free radical species rather than only acting as a pure hydroxyl radical scavenger. Future work in identification of this new radical species may provide more clues to the anti-inflammatory and anti-cancer activity of 5-ASA in preventing the evolution and acquisition of colorectal carcinoma and decreasing the morbidity and mortality associated with this detrimental disease.

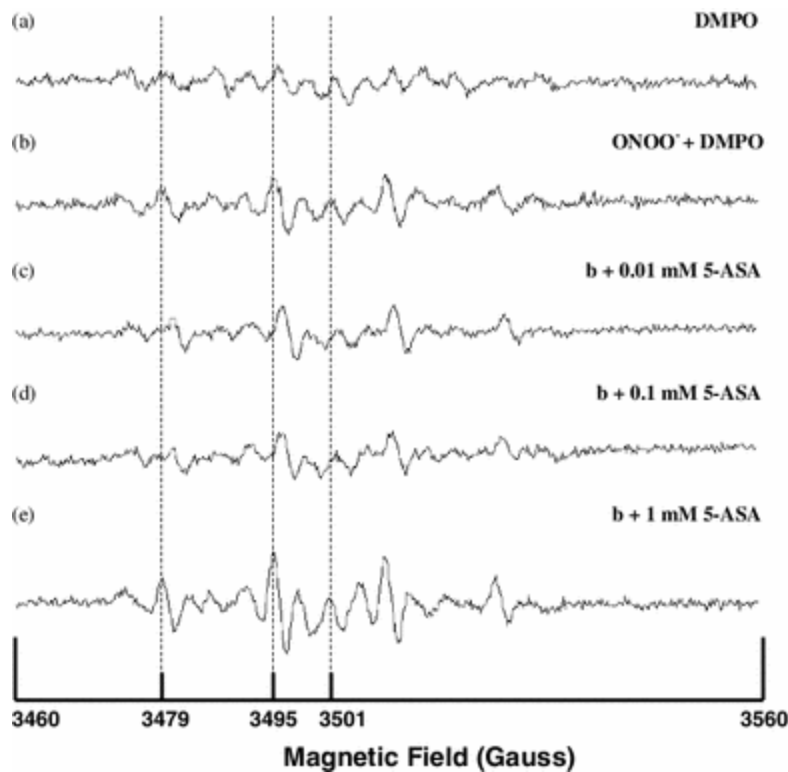


Fig. 8 EPR evidence of the ability of 5-ASA to scavenge peroxynitrite-mediated free radical generation. EPR spectroscopy in combination with spin trap DMPO and peroxynitrite was used to investigate the free radical-scavenging ability of 5-ASA. EPR spectra were recorded for 400 s after the initiation of a reaction containing 3 M DMPO and the following concentrations of 5-ASA and peroxynitrite: *line a*, 3 M DMPO without peroxynitrite and 5-ASA; *line b*, 3 M DMPO + 250 μ M peroxynitrite only; *line c*, 3 M DMPO + 250 μ M peroxynitrite + 0.01 mM 5-ASA; *line d*, 3 M DMPO + 250 μ M peroxynitrite + 0.1 mM 5-ASA; *line e*, 3 M DMPO + 250 μ M peroxynitrite + 1.0 mM 5-ASA. The EPR spectrometer settings were as follows: 86 kHz, X band microwave frequency, 9.8 GHz; microwave power, 29.8 mW (milliWatts); modulation amplitude, 2.17 G (gauss); time constant, 5.1 ms; scan time, 400 s; and receiver gain, 1.78×10^5 . EPR, electron paramagnetic resonance; DMPO, 5,5-dimethylpyrroline-*N*-oxide

In summary, this study demonstrates for the first time that 5-ASA is able to protect against the peroxynitrite-mediated oxidative DNA strand breaks and inhibit peroxynitrite-mediated luminol chemiluminescence. Extensive evidence suggests that peroxynitrite is involved in the mucosa pathology associated with evolution of chronic inflammation and colorectal carcinoma. Thus, the protective effects of 5-ASA on peroxynitrite-mediated oxidative DNA damage may shed some light on the mechanism(s) of its protective activities against inflammation-mediated colorectal carcinoma when used at pharmacologically relevant concentrations observed in human clinical trials and animal models [7].

References

1. Choi CH, Kim YH, Kim YS, Ye BD, Lee KM, Lee BI, Jung SA, Kim WH, Lee H (2012) Guidelines for the management of ulcerative colitis. *Korean J Gastroenterol* 59:118–140
2. Merchea A, Wolff BG, Dozois EJ, Abdelsattar ZM, Harmsen WS, Larson DW (2012) Clinical features and oncologic outcomes in patients with rectal cancer and ulcerative colitis: a single-institution experience. *Dis Colon Rectum* 55:881–885
3. Kulaylat MN, Dayton MT (2010) Ulcerative colitis and cancer. *J Surg Oncol* 101:706–712
4. Jemal A, Center MM, DeSantis C, Ward EM (2010) Global patterns of cancer incidence and mortality rates and trends. *Cancer Epidemiol Biomarkers Prev* 19:1893–1907
5. Fitzpatrick FA (2001) Inflammation, carcinogenesis and cancer. *Int Immunopharmacol* 1:1651–1667
6. Shacter E, Weitzman SA (2002) Chronic inflammation and cancer. *Oncology (Williston Park)* 16:217–226, 229 discussion 230–212
7. Tang J, Sharif O, Pai C, Silverman AL (2010) Mesalamine protects against colorectal cancer in inflammatory bowel disease. *Dig Dis Sci* 55:1696–1703
8. Lyakhovich A, Gasche C (2010) Systematic review: molecular chemoprevention of colorectal malignancy by mesalazine. *Aliment Pharmacol Ther* 31:202–209
9. Velayos FS, Terdiman JP, Walsh JM (2005) Effect of 5-aminosalicylate use on colorectal cancer and dysplasia risk: a systematic review and metaanalysis of observational studies. *Am J Gastroenterol* 100:1345–1353
10. Lyakhovich A, Gasche C (2010) Systematic review: molecular chemoprevention of colorectal malignancy by mesalazine. *Aliment Pharmacol Ther* 31:202–209
11. Ischiropoulos H, Beckman JS (2003) Oxidative stress and nitration in neurodegeneration: cause, effect, or association? *J Clin Invest* 111:163–169
12. Deliconstantinos G, Villiotou V, Stavrides JC, Salemes N, Gogas J (1995) Nitric oxide and peroxynitrite production by human erythrocytes: a causative factor of toxic anemia in breast cancer patients. *Anticancer Res* 15:1435–1446
13. Fraszczak J, Trad M, Janikashvili N, Cathelin D, Lakomy D, Granci V, Morizot A, Audia S, Micheau O, Lagrost L, Katsanis E, Solary E, Larmonier N, Bonnotte B (2010) Peroxynitrite-dependent killing of cancer cells and presentation of released tumor antigens by activated dendritic cells. *J Immunol* 184:1876–1884

14. Rachmilewitz D, Stamler JS, Karmeli F, Mullins ME, Singel DJ, Loscalzo J, Xavier RJ, Podolsky DK (1993) Peroxynitrite-induced rat colitis—a new model of colonic inflammation. *Gastroenterology* 105:1681–1688
15. Beckman JS, Koppenol WH (1996) Nitric oxide, superoxide, and peroxynitrite: the good, the bad, and ugly. *Am J Physiol* 271:C1424–C1437
16. Szabo C (2003) Multiple pathways of peroxynitrite cytotoxicity. *Toxicol Lett* 140–141:105–112
17. Szabo C, Ohshima H (1997) DNA damage induced by peroxynitrite: subsequent biological effects. *Nitric Oxide* 1:373–385
18. Cao Z, Li Y (2004) Potent inhibition of peroxynitrite-induced DNA strand breakage by ethanol: possible implications for ethanol-mediated cardiovascular protection. *Pharmacol Res* 50:13–19
19. Shirai K, Okada T, Konishi K, Murata H, Akashi S, Sugawara F, Watanabe N, Arai T (2012) Bicarbonate plays a critical role in the generation of cytotoxicity during SIN-1 decomposition in culture medium. *Oxid Med Cell Longev* 2012:326731
20. Li Y, Trush MA (1993) DNA damage resulting from the oxidation of hydroquinone by copper: role for a Cu(II)/Cu(I) redox cycle and reactive oxygen generation. *Carcinogenesis* 14:1303–1311
21. Cai L, Klein JB, Kang YJ (2000) Metallothionein inhibits peroxynitrite-induced DNA and lipoprotein damage. *J Biol Chem* 275:38957–38960
22. Kim SY, Lee JH, Yang ES, Kil IS, Park JW (2003) Human sensitive to apoptosis gene protein inhibits peroxynitrite-induced DNA damage. *Biochem Biophys Res Commun* 301:671–674
23. Pascual C, Reinhart K (1999) Effect of antioxidants on induction time of luminol luminescence elicited by 3-morpholinosydnonimine (SIN-1). *Luminescence* 14:83–89
24. Radi RA, Rubbo H, Prodanov E (1989) Comparison of the effects of superoxide dismutase and cytochrome c on luminol chemiluminescence produced by xanthine oxidase-catalyzed reactions. *Biochim Biophys Acta* 994:89–93
25. Thorpe GH, Kricka LJ (1986) Enhanced chemiluminescent reactions catalyzed by horseradish peroxidase. *Methods Enzymol* 133:331–353
26. Radi R, Cosgrove TP, Beckman JS, Freeman BA (1993) Peroxynitrite-induced luminol chemiluminescence. *Biochem J* 290(Pt 1):51–57

27. Szabo C, Ischiropoulos H, Radi R (2007) Peroxynitrite: biochemistry, pathophysiology and development of therapeutics. *Nat Rev Drug Discov* 6:662–680
28. Frejaville C, Karoui H, Tuccio B, Le Moigne F, Culcasi M, Pietri S, Lauricella R, Tordo P (1995) 5-(Diethoxyphosphoryl)-5-methyl-1-pyrroline *N*-oxide: a new efficient phosphorylated nitron for the in vitro and in vivo spin trapping of oxygen-centered radicals. *J Med Chem* 38:258–265
29. Pieper GM, Felix CC, Kalyanaraman B, Turk M, Roza AM (1995) Detection by ESR of DMPO hydroxyl adduct formation from islets of langerhans. *Free Radic Biol Med* 19:219–225
30. Stolze K, Udilova N, Nohl H (2000) Spin trapping of lipid radicals with DEPMPO-derived spin traps: detection of superoxide, alkyl and alkoxy radicals in aqueous and lipid phase. *Free Radic Biol Med* 29:1005–1014
31. Jia Z, Zhu H, Vitto MJ, Misra BR, Li Y, Misra HP (2009) Alpha-lipoic acid potently inhibits peroxynitrite-mediated DNA strand breakage and hydroxyl radical formation: implications for the neuroprotective effects of alpha-lipoic acid. *Mol Cell Biochem* 323:131–138